Proc. 2003 European Microwave Conf., Munich, Germany, Oct. 2003, pp. 1011-1014. Presented by Dominique Schreurs.

RF Behavioural Modelling from Multisine Measurements: Influence of Excitation Type

D. Schreurs[1], M. Myslinski[1], and K. A. Remley[2]

[1] K.U.Leuven, Div. ESAT-TELEMIC, Kasteelpark Arenberg 10, B-3001 Leuven, Belgium
E-mail: Dominique.Schreurs@esat.kuleuven.ac.be; Phone: +32-16-321821; Fax: +32-16-321986
[2] NIST, RF Electronics Group, 325 Broadway, Boulder, CO 80305-3328, USA
Work partially supported by an agency of the U.S. government. Not subject to U.S. copyright.

Abstract **— Behavioural models for RF devices are typically based on large-signal RF measurements. Until now, those measurements were usually limited to single-tone excitations. In this work, we focus on the use of multisines in the experiment design, and, more specifically, evaluate four types of multisine excitations with respect to their ability to generate accurate models. From our analysis, based on experimental results, we can conclude that a multisine excitation with a constant amplitude spectrum and a random phase spectrum is the most appropriate for obtaining accurate behavioural models.**

I. INTRODUCTION

Interest in behavioural modelling has increased because it allows for the representation of not only simple devices such as transistors, but also of circuits, because an equivalent-circuit model is not required. Several behavioural modelling approaches have already been reported in literature, e.g., [1-3]. They typically make use of large-signal measurements that characterize the D.U.T.'s response to single-tone excitations. Recently, we have shown that, with regard to behavioural modelling, a multisine excitation can replace many single-tone excitations, and consequently that it renders the experiment design more efficient [4]. Whereas we focused in [4] on just one multisine type (constant amplitude and phase spectra), the purpose of this study is to investigate the effect of the multisine type on the accuracy and validity range of RF behavioural models. Related considerations have already been addressed in the literature, although, to the authors' knowledge, the applications were limited to low carrier frequencies (hertz or kilohertz range); and the shape of either the amplitude or phase spectrum was also investigated [5-7]. In this work, we treat the modelling of RF devices starting from real large-signal measurements [8], and we look at the design of the amplitude and phase spectrum combined.

In this study, we consider four types of multisine excitations: a multisine with a constant-amplitude and constant-phase spectrum (abbreviated by CC), a constant-magnitude and random-phase spectrum (CR), a constant-magnitude and Schroeder-phase spectrum [9] (CS), and finally a random-magnitude and random-phase spectrum (RR). In an earlier work [10], we showed that the envelope of the CS multisine best approximates a QPSK digitally modulated signal. In this work, we investigate which multisine type is most appropriate from the modelling point of view.

In Section II, we review our state space modelling approach, and discuss the importance of the multisine type. Results from measurements on an amplifier are presented and analyzed in Section III, followed by conclusions in Section IV.

II. STATE SPACE COVERAGE BY MULTISINES

We developed a behavioural modelling method that makes use of the time-domain format of vectorial large-signal measurements [3,4]. The principle is that a two-port RF device, that exhibits no long-term memory effects, can be described by the dynamical equations

$$I_1(t) = f_1\left(V_1(t), V_2(t), \dot{V}_1(t), \dot{V}_2(t), \ddot{V}_1(t), \cdots, \dot{I}_1(t), \dot{I}_2(t)\right) \quad (1)$$

and

$$I_2(t) = f_2\left(V_1(t), V_2(t), \dot{V}_1(t), \dot{V}_2(t), \ddot{V}_1(t), \cdots, \dot{I}_1(t), \dot{I}_2(t)\right), \quad (2)$$

with $I_i(t)$ the terminal currents, and $V_i(t)$ the terminal voltages. The superscript dots denote (higher-order) time derivatives. An alternative to the above equations would be to express the scattered travelling voltage waves b_1 and b_2 as functions of the incident waves a_1 and a_2, and the necessary derived state variables (such as the time derivatives of a_1 and a_2).

The purpose is to determine the number of required state variables, and subsequently the functions $f_1(.)$ and $f_2(.)$. The former can be accomplished by techniques based on the false-nearest-neighbour approach [3]. The latter is a function-fitting problem by which an analytical formulation is selected, e.g., artificial neural networks (ANNs), whose parameters are found by optimisation [4].

The first step in the modelling process is to collect the data from measurements. In Ref. [4], we presented an approach to efficiently handle multisine data in time-domain representation. In order to evaluate and compare the four multisine types considered, we carried out an experiment by which we kept the total incident average voltage across the modulation bandwidth constant for the four considered cases. The number of tones was nine, the RF carrier frequency was 800 MHz, and the offset frequency between the tones was 200 kHz. We applied these excitations to an off-the-shelf amplifier and measured the voltages and currents at both the input (port 1) and output (port 2). The time-domain waveforms of $V_2(t)$ are shown in Fig. 1 for the four cases. One IF period is plotted, which encompasses many RF periods (on the

nanosecond scale). We notice that only one situation of the random CR and RR cases is considered. Although the instantaneous values might vary due to the actual values of the random variables, the trends are maintained.

From Fig. 1, we notice that the CC case reaches high amplitudes, although for a short time period. In the CS case, the maximal voltage is moderate, and this value is reached by the majority of the RF periods. In the CR case, the maximal voltage swing is moderate as well, but we have a better variation in maximal/minimal values that are reached over the RF periods. In the RR case, the maximal voltage value is higher again, but also the maximal/minimal amplitude is quite small over a considerable number of RF periods. The importance of these RF amplitude variations will become clear in the following.

Note that in our modelling approach, the relationships expressed by equations (1) and (2) are determined over a state space range that is representative for the D.U.T. As the main state variables in our formalism are the terminal voltages, we plot the covered (V_1,V_2) state spaces for the four cases in Fig. 2. Here we plot the time-domain waveform of $V_2(t)$ as a function of the time-domain waveform of $V_1(t)$. Plotting these waveforms would result in a big black spot due to the high number of required sample points needed to meet the Nyquist criterion. Thus, we sample the IF period equidistantly in time and consider one RF period at each of these samples [4].

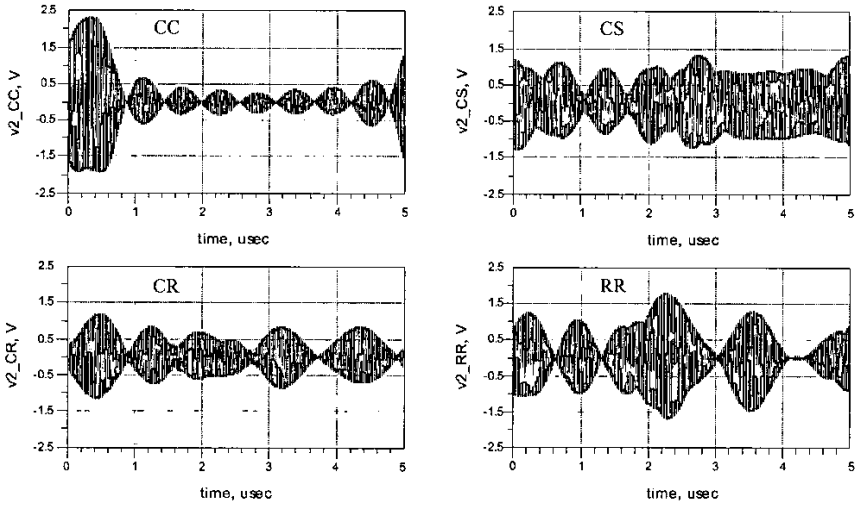

Fig. 1. Measured $V_2(t)$ for the four multisine types: CC (top left), CS (top right), CR (bottom left), and RR (bottom right).

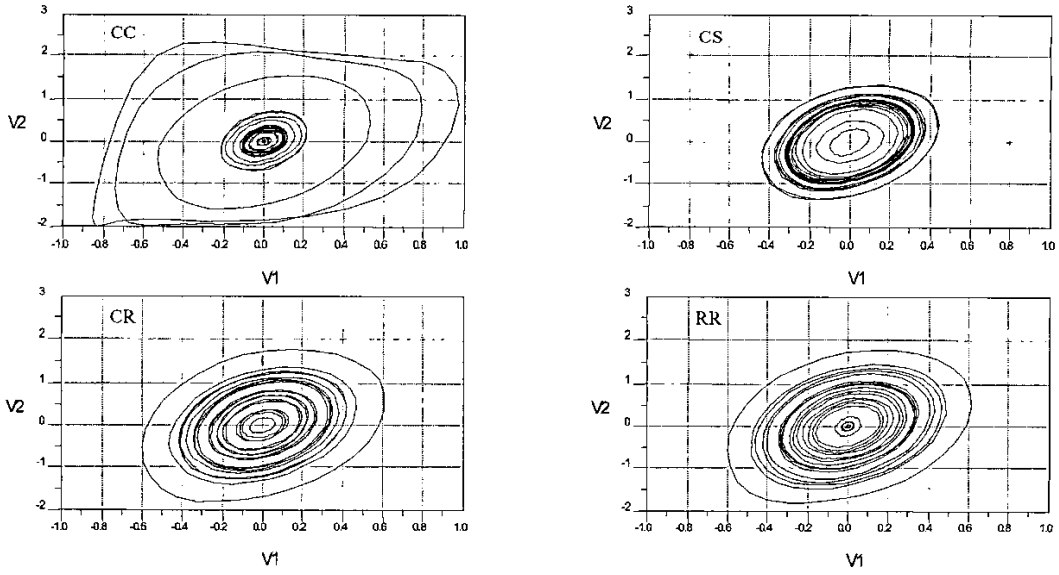

Fig. 2. (V_1,V_2) coverage (in [V]), represented by 20 RF periods, corresponding to an equidistantly sampled IF period: CC (top left), CS (top right), CR (bottom left) and RR (bottom right).

Table 1. Measured results and corresponding absolute differences between predictions by the four models and measurements, and this for b_1 and b_2 at 800.0 MHz and at 800.8 MHz. The excitation is a large-amplitude 17-tone CS multisine.

	MAG					PHASE				
	Meas.	Abs. errors [dB] by model case:				Meas.	Abs. errors (deg.) by model case:			
	[dBm]	CC	CS	CR	RR	[deg.]	CC	CS	CR	RR
$b_{1,800.0MHz}$	-24.39	0.18	-0.02	-0.24	0.04	107.59	-0.65	-0.12	-0.27	-0.05
$b_{1,800.8MHz}$	-24.10	0.17	-0.18	-0.17	-0.12	164.89	-0.11	0.63	0.08	0.57
$b_{2,800.0MHz}$	0.93	-0.04	-0.09	-0.05	-0.06	-82.95	-0.08	-0.64	-0.51	-0.48
$b_{2,800.8MHz}$	1.02	-0.15	-0.13	-0.16	-0.14	-26.88	1.17	0.88	0.62	0.54

Table 2. Measured results and corresponding absolute differences between predictions by the four models and measurements, and this for b_2 at 799.0991 MHz. The excitation is a large-amplitude 17-tone CS multisine.

	MAG					PHASE				
	Meas.	Abs. errors [dB] by model case:				Meas.	Abs. errors (deg.) by model case:			
	[dBm]	CC	CS	CR	RR	[deg.]	CC	CS	CR	RR
$b_{2,799.0991MHz}$	-40.91	5.92	2.68	0.59	0.25	-131.64	21.20	-11.96	11.67	33.84

Table 3. Measured results and corresponding absolute differences between predictions by the four models and measurements, and this for b_1 and b_2, as measured at 800.0 MHz and 800.8 MHz. The excitation is a low-amplitude 17-tone CS multisine.

	MAG					PHASE				
	Meas.	Abs. errors [dB] by model case:				Meas.	Abs. errors (deg.) by model case:			
	[dBm]	CC	CS	CR	RR	[deg.]	CC	CS	CR	RR
$b_{1,800.0MHz}$	-34.07	-0.13	-0.04	0.01	-0.03	83.08	0.62	0.05	-0.23	0.04
$b_{1,800.8MHz}$	-34.12	-0.07	0.02	0.07	0.04	113.14	-0.02	-0.11	-0.69	-0.33
$b_{2,800.0MHz}$	-8.54	0.04	-0.09	-0.01	-0.05	-108.79	-0.15	0.99	0.37	0.72
$b_{2,800.8MHz}$	-8.43	-0.10	-0.16	-0.08	-0.12	-79.46	1.60	1.50	0.39	0.78

Table 4. Measured results and corresponding absolute differences between predictions by the four models and measurements, and this for b_1 and b_2, as measured at 800.0 MHz and 800.8 MHz. The excitation is a phase-detrended 17-tone CS multisine.

	MAG					PHASE				
	Meas.	Abs. errors [dB] by model case:				Meas.	Abs. errors (deg.) by model case:			
	[dBm]	CC	CS	CR	RR	[deg.]	CC	CS	CR	RR
$b_{1,800.0MHz}$	-24.39	0.18	-0.02	0.03	0.04	-141.68	-0.58	0.17	-0.29	-0.06
$b_{1,800.8MHz}$	-24.10	0.17	-0.17	-0.17	-0.12	-98.80	-0.15	0.61	0.08	0.56
$b_{2,800.0MHz}$	0.93	-0.07	-0.09	-0.05	-0.06	27.78	-0.06	-0.21	-0.50	-0.50
$b_{2,800.8MHz}$	1.02	-0.15	-0.11	-0.16	-0.14	69.42	1.23	0.90	0.62	0.54

From the plots, we can deduce that the (V_1,V_2) coverage of the CC case is the largest, and that of the CS case is the smallest. We notice however only few RF trajectories towards the extreme voltage values in the CC case because, as indicated above, the larger values are reached over only a small part of the IF period. When considering the other cases, we observe that the smaller voltage values are not as well covered in the CS case and there is a 'gap' in the RR case. We could cover those sections better by changing the excitation conditions, but for the comparison we choose to keep the total average input voltage constant. As a result, we conclude that the CR coverage looks the best for the experimental conditions considered. In the next Section, we will show how this observation propagates to modelling accuracy.

III. Behavioural Modelling Results

After collecting the measured data, we constructed a behavioural model for the off-the-shelf amplifier according to the four cases, using the procedure described in [4]. Its basic principle is that the model is a composite set of models, one corresponding to each RF trajectory. The overall model's representation is an artificial neural network with one hidden layer.

To check the models' accuracy, we compare model predictions to measurements that are different from the ones used in the modelling process. The test excitation was a 17-tone multisine signal with an offset frequency of 100 kHz and with a constant amplitude and Schroeder phase spectrum. Note that we checked separately that the selected off-the-shelf amplifier exhibits no or very little long-term memory effects. Table 1 lists the differences between predictions and measurements of the waves b_1 and b_2 at two of the fundamental tones (800.0 MHz, at the center of the band, and 800.8 MHz, at the edge). Table 2 lists the b_2 results at an intermodulation product frequency. The corresponding b_1 results are not shown, because the values are very small (below –60 dBm).

From these tables, we can deduce that the model predictions are close to measured values. Since differences in model predictions for the fundamental tones are small, we mainly focus on the comparison of the intermodulation product results in Table 2. The CR and RR cases both predict the magnitude well, but the phase prediction of the RR case deviates from the measurement. The CC case performs worst in terms of the magnitude. To explain this, we have to take into account the (V_1,V_2) area as covered by the models (Fig. 2). The instantaneous V_1 and V_2 values of this 17-tone experiment (not shown)

vary respectively between –0.5 V and 0.65 V, and between –1.6 V and 1.7 V. From Fig. 2 we notice that this corresponds well with the ranges covered by the CR and RR models. The CS model gets extrapolated towards the extreme-voltage values, while the CC model gets interpolated, due to its few trajectories, and subsequently less training information, near the extreme values of the area covered by this experiment. From this analysis, we can conclude that there is a clear correlation between the accuracy of the models and how the state space is covered (dense or sparse). Since the trajectories of the CR case are the most uniformly spread as compared to the other cases, this multisine type yields the best overall model. Even though the phases are distributed randomly, we expect that this uniform spread will be maintained, especially for greater numbers of tones. On the other hand, pointing out the multisine type that yields the worst model is not straightforward because this depends strongly on how the excitation at which the models get evaluated 'populates' the state space.

The results of a second example are summarized in Table 3. This time, the models are evaluated with a low-amplitude 17-tone CS excitation. The instantaneous V_1 and V_2 voltage values vary respectively between -0.2 V and 0.2 V, and between –0.55 V and 0.6 V. As this area is well covered by the CC and CR cases, their predictions are very good. The CS and RR results are very similar, although these models get interpolated to a greater degree. The density of their trajectories is apparently sufficient such that the evaluation of the ANN on points in between trajectories still yields highly accurate results. No intermodulation product results are listed, because their levels are very low (below –60 dBm).

The data presented above were RF calibrated but not phase de-trended. This means that there is still an unknown delay between the signal source and the reference plane of interest that shifts the position of the signal envelope over time. By applying the method developed in [11], this unknown delay can be estimated, and all measured data can be corrected accordingly. As a result, the maximum of the signal envelope could be, for example, aligned to time zero. Since the correction ensures that the interrelationships between all signals are maintained and that the state space coverage remains identical, this phase de-trending process should not affect the modelling. This is confirmed by Table 4 which represents the same case as Table 1, but with the different models now evaluated with a phase-detrended 17-tone excitation. As expected, there is no noticeable change in the predicted amplitude values; moreover, the models manage to predict the corrected phases with a similar accuracy as in the case of the non phase-detrended data.

IV. CONCLUSIONS

We compared four multisine excitation types with respect to their ability to yield accurate RF behavioural models. We have shown that there is a clear correlation between the model accuracy and how the state space is covered (dense or sparse). For the experimental conditions considered, the RF trajectories of the multisine with a constant amplitude and random phase spectrum are the most uniformly spread, and so this multisine type yields the best overall model. Finally, we can conclude that the multisine type that is most appropriate for approximating digitally modulated excitations is not automatically also the best candidate to be used in experiment design for model building.

ACKNOWLEDGEMENT

D. Schreurs is supported by the Fund for Scientific Research-Flanders as a post-doctoral fellow.

REFERENCES

[1] J. Verspecht, F. Verbeyst, M. Vanden Bossche, and P. Van Esch, "System level simulation benefits from frequency domain behavioral models of mixers and amplifiers", *European Microwave Conf.*, 1999, pp. 29-32.

[2] T. Wang and T. Brazil, "The estimation of Volterra transfer functions with applications to RF power amplifier behavior evaluation for CDMA digital communication", *IEEE Int. Microwave Symp.*, 2000, pp. 425-428.

[3] D. Schreurs, N. Tufillaro, J. Wood, D. Usikov, L. Barford, and D.E. Root, "Development of time domain behavioural non-linear models for microwave devices and ICs from vectorial large-signal measurements and simulations", *European Gallium Arsenide and related III-V compounds Applications Symp.*, 2000, pp. 236-239.

[4] D. Schreurs and K. Remley, "Use of multisine signals for efficient behavioural modelling of RF circuits with short-memory effects", *Automatic RF Techniques Group Conf.*, June 2003, pp. 65-72.

[5] A. McCormack, K. Godfrey, and J. Flower, "Periodic signal designs for nonlinear system identification", *IEEE Instrumentation and Measurement Technology Conf.*, 1995, pp. 265-270.

[6] J. Schoukens and T. Dobrowiecki, "Design of broadband excitation signals with a user imposed power spectrum and amplitude distribution", *IEEE Instrumentation and Measurement Technology Conf.*, 1998, pp. 1002-1005.

[7] P. Crama and J. Schoukens, "Initial estimates of Wiener and Hammerstein systems using multisine excitation", *IEEE Trans. Instrum. Meas.*, Vol. 50, No. 6, pp. 1791-1795, 2001.

[8] J. Verspecht, P. Debie, A. Barel, and L. Martens, Accurate on wafer measurement of phase and amplitude of the spectral components of incident and scattered voltage waves at the signal ports of a nonlinear microwave device, *IEEE Int. Microwave Symp.*, 1995, pp. 1029-1032.

[9] R. Pintelon and J. Schoukens, *System identification: A frequency domain approach*, publisher IEEE press, 2001.

[10] K. A. Remley, "Multisine excitation for ACPR measurements", *IEEE Int. Microwave Symp.*, 2003, pp. 2241-2144.

[11] K. Remley, D. Williams, D. Schreurs, G. Loglio, and A. Cidronali, "Phase Detrending for Measured Multisine Signals", *Automatic RF Techniques Group Conf.*, June 2003, pp. 73-83.